Suplemento de la Revista Mexicana de Física **4** 021124 (2023) 1–7

Evolution of pion mass with temperature

J. L. Flores-Pon[a], M. A. Bedolla[a], P. Sloane[a], and A. Raya[b]

[a]*Facultad de Ciencias en Física y Matemáticas (FCFM), Universidad Autónoma de Chiapas, Carretera Zapata Km. 8, Rancho San Francisco, Tuxtla Gutiérrez 29050, Chiapas, México.*
[b]*Instituto de Física y Matemáticas, Universidad Michoacana de San Nicolás de Hidalgo, Edificio C-3, Ciudad Universitaria, 58040, Morelia, Michoacán, México.*

Received 18 March 2023; accepted 13 April 2023

We study the evolution of light quarks with isospin symmetry and the pion masses in the presence of a thermal bath and study their temperature dependence. In addition, we analyze the inclusion of a coupling with temperature dependence. We attempt to study the dissolution of bound-states at temperatures higher than the critical temperature, but we found that the model shows that the bound-state's mass increases. We base our study on a momentum-independent symmetry-preserving truncation scheme contact interaction in the Schwinger-Dyson equations framework.

Keywords: Contact interaction; finite temperature; bound-states dissolution.

DOI: https://doi.org/10.31349/SuplRevMexFis.4.021124

1. Motivation

Quantum chromodynamics (QCD) is the quantum field theory of strong interactions between quarks and gluons. These interactions produce bound-states known has hadrons, which are the particles that can be found in nature. One of the particularities of this theory is that its main ingredients, the quarks, cannot be found as free particles in nature: the quarks are confined. Confinement is an emergent phenomenon which appears in the regime of low energies in the theory, where chiral symmetry is dynamically broken and quarks acquire dynamical mass, which is responsible for 98% of the visible mass of Universe. On the other hand, in the regime of high energies, asymptotic freedom manifests itself, the running coupling becomes small enough and it is possible to use perturbation theory [1–3]. In this region, quarks behave as free particles.

In particular, the behavior of QCD is affected if quarks are in the presence of heat baths or magnetic fields. At low temperatures, bound-states continue to be color-singlet hadrons, whereas at high temperatures, the interaction gets increasingly screened and weak, and this restores the chiral symmetry of quarks because the coupling decreases. Thus, the behavior of quarks and gluons suggest asymptotic freedom. This behavior has been widely studied in literature, see for example Refs. [4–13] for lattice QCD, Refs. [14–24] for works based upon continuum techniques of the Schwinger-Dyson equations (SDEs), and Refs. [25–28] within the Chiral Perturbation Theory Framework.

There are other studies that consider variation of color and flavor numbers to study the restoration of chiral symmetry breaking confinement and resulting in deconfinement, others that study the quark gap equation under the presence of strong magnetic fields, which favors the generation of dynamic mass for any value of the coupling strength. This phenomenon was first studied in quantum electrodynamics (QED) and was called magnetic catalysis [29–35]. If we consider a coupling that decreases with larger magnetic fields, the restoration of chiral symmetry pops up and the phenomena of inverse magnetic catalysis appears catalysis [24, 36–40]. A recent work [41] indicates that an electric field favors the restoration of chiral symmetry.

Moreover, it is known that a quark-gluon plasma has been produced at the relativistic heavy ion collider (RHIC) [42]. This plasma behaves as a nearly perfect fluid if the temperature of the system is larger than the critical temperature required for its creation: $T_c < T$ [43]. At this point, the collective excitations of gluons and quarks should prevail above the excitation of individual free gluons and quarks. It is possible to study this phenomena by studying the screening masses of hadrons above the critical temperature T_c [44], because the long-range structure of a plasma determines quantities such as its equation of state and transport properties [18].

However, in most of the studies done in Lattice [45–47], it is shown that strong correlations persist above the critical temperature, $T > T_c$; and, a larger mass of bound-states appears as an associated screening masses, and the parity-partner states become degenerate. There are some proposals that suggests that the inertial masses of light-quark bound-states may vanish at the deconfinement temperature; and that this could be a signal of bound-state dissolution [18].

In this work, we study the quark mass equation in the presence of a thermal bath. With this computed mass, we calculate the pion mass as a function of temperature. Later we consider a coupling which becomes smaller with temperature. The detailed analysis and discussions are found in Refs. [18, 24]. Here, we outline the general expressions and describe how the results can be obtained.

2. Pion at zero temperature

We start by presenting the generalities of the contact interaction (CI) for the quark gap equation.

In this simple yet effective model, [48–52], it is assumed that the quark-gluon interaction is effectively the symmetry-preserving vector-vector CI leading to a constant gluon propagator:

$$g^2 D_{\mu\nu}(k) = \frac{4\pi\alpha_{\rm IR}}{m_G^2}\delta_{\mu\nu} \equiv \alpha_{\rm eff}\delta_{\mu\nu}, \tag{1}$$

$$\Gamma^a_\mu(p,q) = \frac{\lambda^a}{2}\gamma_\mu, \tag{2}$$

where $m_G = 800\,$MeV is a gluon mass scale generated dynamically in QCD [53], and $\alpha_{\rm IR}$ is the CI model parameter, which can be interpreted as the interaction strength in the infrared region [54, 55]. Replacing the full quark-gluon vertex by its bare counterpart completes the definition of the model. As a consequence, a constant mass function is obtained. Since it is necessary to solve divergent integrals, a regularization procedure should be adopted. To regularize the integrals in the CI model, the proper time regularization scheme [56] is adopted. This leads to a quark propagator of the type:

$$S_f^{-1}(p) = i\gamma\cdot p + M_f\,, \tag{3}$$

with a constant dressed quark mass.

$$M_f = m_f + \alpha_{\rm eff}\frac{M_f^3}{8\pi^2}\Gamma(-1,\tau_{\rm UV}M_f^2,\tau_{\rm IR}M_f^2)\,, \tag{4}$$

where $m_f = m_u = m_d$ is the light-quark current-mass, and $\Gamma(a,z_1,z_2)$ is the generalized incomplete Gamma function:

$$\Gamma(a,z_1,z_2) = \Gamma(a,z_1) - \Gamma(a,z_2)\,. \tag{5}$$

The parameters $\tau_{\rm IR}$ and $\tau_{\rm UV}$ are infrared and ultraviolet regulators, respectively. A nonzero value for $\tau_{\rm IR} \equiv 1/\Lambda_{\rm IR}$ implements confinement by ensuring the absence of the quark production threshold [57]. On the other hand, since the CI model provided by Eq. (1) represents a non-renormalizable theory, so $\tau_{\rm UV} \equiv 1/\Lambda_{\rm UV}$ cannot be removed, it becomes part of the model and sets the scale for all dimensional quantities. Additionally, the ultraviolet cutoff also plays an important role in studying heavier quarks: increasing $\Lambda_{\rm UV}$ mimics the short-distance effects as the quark mass increases [49, 58].

TABLE I. Quark u current mass m_u, dynamic mass computed from the gap equation for u current mass and chiral limit $m_u = 0$, and pion mass computed from the Bethe-Salpeter equation at $T = 0$. The results are obtained with $\alpha_{\rm IR} = 0.93\pi$ and (in GeV) $\Lambda_{\rm ir} = 0.24$, $\Lambda_{\rm uv} = 0.905$. (These parameters take the values determined in the spectrum calculation of Ref. [48]; isospin symmetry is assumed).

m_u	M_0	M	m_π
0.007 GeV	0.356 GeV	24.3 GeV	0.140 GeV

Mesons are studied through the Bethe-Salpeter equation, the relativistic bound-state problem for hadrons. This equation is characterized by two valence-quarks [59],

$$[\Gamma(k;P)]_{tu} = \int\frac{d^4q}{(2\pi)^4}[\chi(q;P)]_{sr}\mathcal{K}^{rs}_{tu}(q,k;P)\,, \tag{6}$$

where $[\Gamma(k;P)]_{tu}$ represents the bound-state BSA and $\chi(q;P) = S(q+P)\Gamma S(q)$ is the BS wave-function; r,s,t,u represent color, flavor and spinor indices; and $\mathcal{K}$ is the relevant quark-antiquark scattering kernel. Equation (6) is an eigenvalue problem: it has a solution for $P^2 = -m_H^2$, where m_H is the mass of any one of the bound-state's at $T = 0$. Solving this equation could be considered as the $T = 0$ values of the quark and mesons masses.

In Table I, we show the $T = 0$ values of M and M_0 computed from Eq. (4) for $m_f = 7$ MeV and $m_f = 0$, and the pion mass m_π obtained from Eq. (6) with the parameters listed there.

3. Pion at finite temperature

A primary feature of QCD is that light-particle creation and annihilation effects occur in its non-perturbative region. In consequence, thinking about computing a potential between two light quarks to form a bound-state is inconceivable [60, 61]. However, we aim to profit from one asset of the DSE framework, which is its ability to treat mesons and baryons on both at zero and nonzero temperature. We explain some details about the computation of pion mass in this section.

3.1. Gap Equation

For instance, within the contact interaction model provided by Eq. (1), the $T \neq 0$ dressed-quark propagator now is obtained from the following gap equation:

$$S^{-1}(\vec{p},\omega_n) = i\vec{\gamma}\cdot\vec{p} + i\gamma_4\omega_n + m_f + \frac{16\pi\alpha_{\rm IR}}{3m_G^2}\int_{l,dq}\gamma_\mu S(\vec{q},\omega_l)\gamma_\mu\,, \tag{7}$$

where $\int_{l,dq} = T\sum_{l=-\infty}^{\infty}\int d^3\vec{q}/(2\pi)^3$ and $\omega_n = (2n+1)\pi T$ is the fermion Matsubara frequency. Luckly its solution is similar to Eq. (3),

$$S^{-1}(\vec{p},\omega_n) = i\vec{\gamma}\cdot\vec{p} + i\gamma_4\omega_n + M_f\,, \tag{8}$$

and the dressed-quark mass function at finite temperature is:

$$M_f = m_f + \frac{2\alpha_{\rm eff}M_f T}{3\pi^{3/2}}\int_{\tau_{\rm UV}^2}^{\widetilde{\tau}_{\rm IR}^2} d\tau\,\frac{{\rm e}^{-M_f^2\tau}\Theta_2(0,{\rm e}^{-(2\pi T)^2\tau})}{\tau^{3/2}}\,, \tag{9}$$

where we have introduced an infrared coupling with temperature dependence

$$\widetilde{\tau}_{\rm IR} = \tau_{\rm IR}\frac{M_f(0)}{M_f(T)}\,, \tag{10}$$

$M_f(0)$ is provided by Eq. (4), which is the dressed-quark mass at $T = 0$ and $\Theta_2(x, y)$ is the second Jacobi Theta Function. With the quark propagator, it is possible to compute the quark-antiquark condensate, which serves as an indicator parameter to determine chiral symmetry breaking. At finite temperature, the condensate reads:

$$-\langle\psi\overline{\psi}\rangle^{\frac{1}{3}} = \frac{3M(T)T}{2\pi^3/2}\int_{\tau_{\rm UV}^2}^{\widetilde{\tau}_{\rm IR}^2} d\tau \times \frac{e^{-M(T)\tau}\Theta_2(0, e^{-4\pi^2T^2\tau})}{\tau^{3/2}}. \quad (11)$$

It has been seen in Ref [49] that a reduction in the coupling is reflected in an increase of the ultraviolet cutoff. Considering this, we see in Eq. (10) that temperature has an effect in the ultraviolet cutoff, $\widetilde{\tau}_{\rm IR}$ increases with temperature. This indicates that the coupling must be a function of temperature. However, the objective of this manuscript is not to derive a coupling with temperature dependence, we just propose a temperature dependence function to determine a variation in the mass function. Thus, we follow a QCD-like approach from Ref. [24], and define

$$\alpha_{\rm eff}(x) = \frac{\alpha_{\rm eff}}{1 + \alpha\ln(1 + \beta x)}, \quad (12)$$

where $\alpha = 1.4$, $\beta = 1.33$, $x = T/\Lambda_{\rm QCD}$, and $\Lambda_{\rm QCD} = 300$ MeV . The parameters α and β are fixed to obtain a reasonable description of the lattice average of up and down quark condensates at $T = 0$. For the objectives of this manuscript, the parameters have been slightly changed to have a notorious decrease in the quark mass function and the quark-antiquark condensate in the region of study (0.0 – 0.3 GeV). Studies with more justified couplings are planned in the near future.

In Fig. 1 we show the evolution with temperature of quark mass function for $m_f = 0.007\,\text{MeV}$ and $m_f = 0\,\text{MeV}$. In both cases, we see a reduction of the dynamic mass after a certain critical temperature. In particular, in the chiral limit it is assured that the confining scale vanishes at the chiral symmetry restoration temperature. This could be interpreted as the transition region of confinement, because the quark shows its current mass.

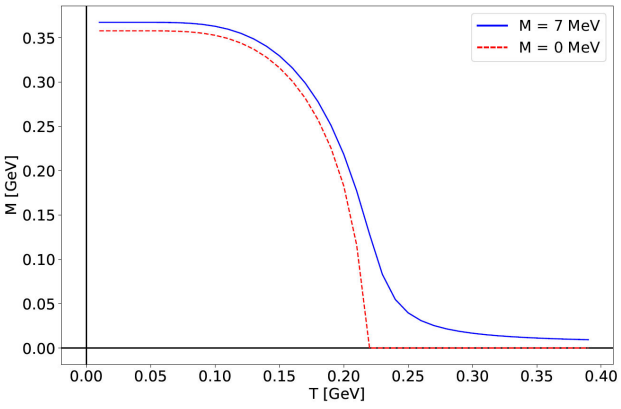

FIGURE 1. Quark Mass Function for $m_f = 7$ MeV and $m_f = 0$.

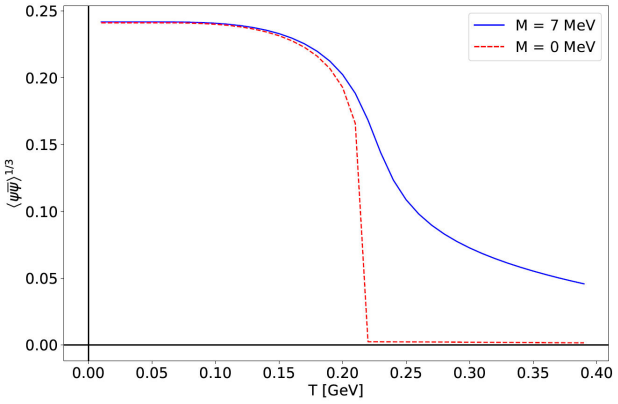

FIGURE 2. Quark-antiquark condensate for $m_f = 7$ MeV and $m_f = 0$.

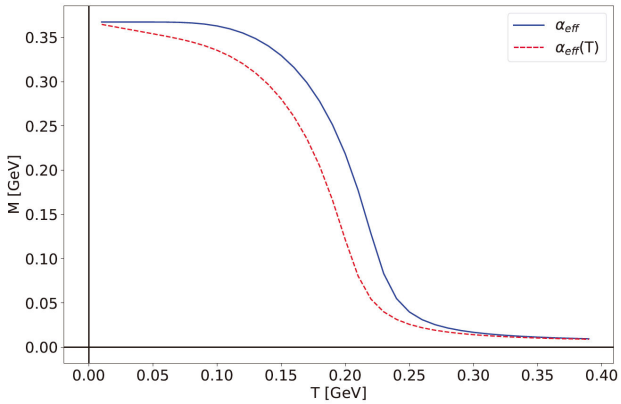

FIGURE 3. Comparison of quark Mass Function for $m_f = 7$ MeV without (solid curve) and with (dashed curve) the coupling given by Eq. (12).

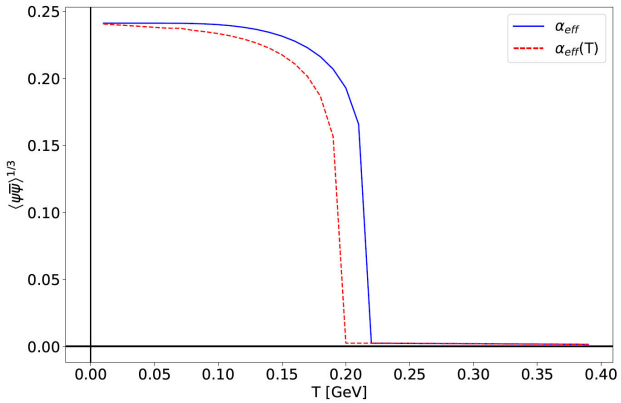

FIGURE 4. Quark-antiquark condensate for $m_f = 0$ MeV without (solid curve) and with (dashed curve) the coupling given by Eq. (12).

This effect is also present in the quark-antiquark condensate, provided by Eq. (11), as shown in Fig. 2. It is notable that in the chiral limit, the condensate vanishes at

the critical temperature, a result that is consistent with Refs. [25, 27, 28, 62, 63]. In Fig. 3, we plot the mass equation for $m_f = 7$ MeV when we include the dependent-temperature coupling given by Eq. (12) and, in Fig. 4, we show the condensate for the chiral limit with and without a temperature dependent coupling. Here, the effect of the coupling is to reduce the critical temperature for chiral restoration.

3.2. Bethe-Salpeter equation

At leading order in the symmetry-preserving truncation scheme of Ref. [64], the Bethe-Salpeter Eq. (6), in the homogeneous rainbow-ladder prescription takes the form,

$$\Gamma_H(P) = -\frac{4\,\alpha_{\rm eff}}{3}\int_{l,dt}\gamma_\mu S(t+P)\Gamma_H(P)S(t)\gamma_\mu\,, \quad (13)$$

where S is obtained from Eq. (7) and $P = \{\vec{P}, 0\}$ is the total momentum entering the amplitude. For this work, we aim to study the behavior of the spatially screening mass, so it is necessary to focus only on the meson's zeroth Matsubara frequency . The rainbow-ladder truncation is known to provide reliable results for the $T = 0$ properties of vector and flavor non-singlet pseudoscalar mesons [65, 66].

The explicit form for the BSE of the π is readily obtained following the procedures described in Refs. [49, 67, 68]. For the pion we found an obvious analogue of Eqs. (A4)–(A6) in Ref. [49]. Herein, $\mathcal{C}_{01}(\mathfrak{M})$ and $\mathcal{C}_{02}(\mathfrak{M})$ are replaced by $\mathcal{C}_{01}(\mathfrak{M};T)$ and $\mathcal{C}_{02}(\mathfrak{M};T)$ respectively. The argument of these functions is:

$$\mathfrak{M} = \mathfrak{M}(M^2,\alpha,Q_0^2) = M^2 + \alpha(1-\alpha)P^2\,. \quad (14)$$

Given these observations, one can readily express the pseudoscalar BSE:

$$\begin{bmatrix} E_\pi(P) \\ F_\pi(P) \end{bmatrix} = \frac{\alpha_{\rm eff}}{3\pi^2}\begin{bmatrix} \mathcal{K}^\pi_{EE} & \mathcal{K}^\pi_{EF} \\ \mathcal{K}^\pi_{FE} & \mathcal{K}^\pi_{FF} \end{bmatrix}\begin{bmatrix} E_\pi(P) \\ F_\pi(P) \end{bmatrix}, \quad (15)$$

where the matrix elements are:

$$\mathcal{K}^\pi_{EE} = \int_0^1 d\alpha\Big[\mathcal{C}_{01}(\mathfrak{M}(M^2,\alpha,-m_\pi^2);T) + 2\alpha(1-\alpha)\,m_\pi^2\,\mathcal{C}_{02}(\mathfrak{M}(M^2,\alpha,-m_\pi^2);T)\Big], \quad (16a)$$

$$\mathcal{K}^\pi_{EF} = -m_\pi^2\int_0^1 d\alpha\,\mathcal{C}_{02}(\mathfrak{M}(M^2,\alpha,-m_\pi^2);T), \quad (16b)$$

$$\mathcal{K}^\pi_{FE} = \frac{1}{2}M^2\int_0^1 d\alpha\,\mathcal{C}_{02}(\mathfrak{M}(M^2,\alpha,-m_\pi^2);T), \quad (16c)$$

$$\mathcal{K}^\pi_{FF} = -2\mathcal{K}_{FE}\,, \quad (16d)$$

and

$$\mathcal{C}_{01}(\mathfrak{M};T) = \int_{\tau^2_{\rm uv}}^{\tau^2_{\rm ir}} d\tau\,{\rm e}^{-\tau\mathfrak{M}}\,2T\vartheta_2({\rm e}^{-\tau 4\pi^2T^2})\frac{\sqrt{\pi}}{\tau^{3/2}}\,, \quad (17)$$

$$\mathcal{C}_{02}(\mathfrak{M};T) = -\frac{d}{d\mathfrak{M}}\mathcal{C}_{01}(\mathfrak{M};T) \quad (18)$$

being $\vartheta_2(x)$ is a Jacobi theta-function [69].

In Fig. 5, we show the evolution with temperature of pion mass with $m_f = 7$ MeV and for the Goldstone boson with $m_f = 0$. We notice that after the critical temperature point, where the bound-state must cease to exist, the mass of the bound-state becomes larger with temperature. This behavior is also present in Lattice studies [45–47], but it is inconsistent with Chiral Perturbation Theory results [26], where the pion mass as a function of temperature gets lower as temperature increases. We will aim to obtain a similar result in a future study. Additionally, we see that its mass, originally zero, becomes larger after the critical temperature point is reached.

Finally, in Fig. 6 we compare the evolution with temperature of pion mass with $m_f = 7$ MeV with and without the temperature-dependent coupling from Eq. (12). We notice that the effect of the temperature-dependent coupling is neg-

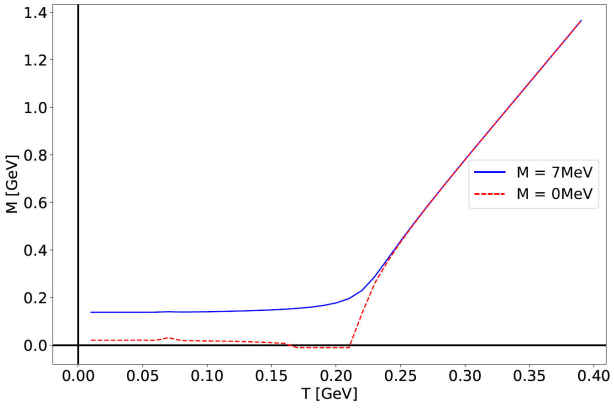

FIGURE 5. Temperature dependence of pion mass with isospin symmetry. The solid curve is for $m_f = 7$ MeV, dash-point curve is for $m_f = 0$. Pion should become massless after certain temperature, that we could relate with a bound-state dissolution. The Goldstone boson should be massless for all temperatures, but its mass increases after the critical temperature.

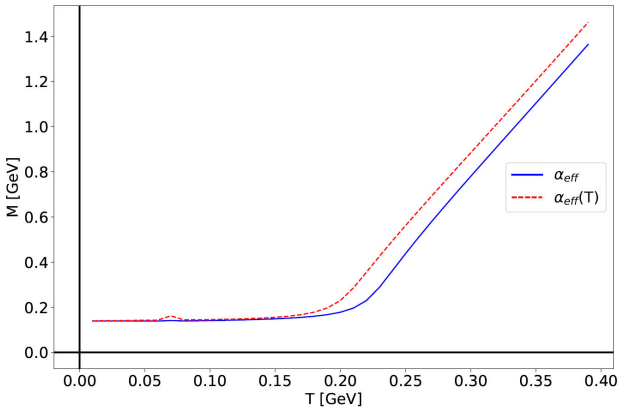

FIGURE 6. Temperature dependence of pion mass with isospin symmetry. The solid curve is for $m_f = 7$ MeV, dashed curve is considering a temperature-dependent coupling Eq. (12). In both cases, the mass increases after the critical temperature point is reached.

ligible on the pion mass. This could be an indication that the coupling strength is not the agent which produces the increase of pion mass after the critical temperature.

4. Conclusions

We studied the effect of temperature of light quark mass dressed and pion masses. We noticed that temperature has the effect of restoring chiral symmetry in the quark mass, leading the quark mass to its current value after the critical temperature is reached. Surprisingly, despite the fact that the quark mass diminishes with temperature, we cannot claim the same about the pion mass. This increases slightly before the critical temperature, and after the critical temperature is reached, its mass increases more drastically. However, this behavior is also present in Lattice studies. In addition, we do not see any improvement in this behavior if we take a temperature-dependent coupling. In the future, we are planning to study the effects of temperatures in the other meson channels: scalar, vector and axial, and we expect to develop a model which could show bound-state dissolution after the critical temperature point.

Acknowledgements

We acknowledge the organizers of XVIII Mexican Workshop of Particles and Fields for an excellent organization.

1. D. J. Gross and F. Wilczek, Ultraviolet Behavior of Nonabelian Gauge Theories, *Phys. Rev. Lett.* **30** (1973) 1343, https://doi.org/10.1103/PhysRevLett.30.1343.
2. H. D. Politzer, Reliable Perturbative Results for Strong Interactions?, *Phys. Rev. Lett.* **30** (1973) 1346 https://doi.org/10.1103/PhysRevLett.30.1346.
3. D. J. Gross and F. Wilczek, Asymptotically Free Gauge Theories - I, *Phys. Rev. D* **8** (1973) 3633 https://doi.org/10.1103/PhysRevD.8.3633.
4. C. Bernard *et al.* [MILC], QCD thermodynamics with three flavors of improved staggered quarks, *Phys. Rev. D* **71** (2005) 034504 https://doi.org/10.1103/PhysRevD.71.034504.
5. M. Cheng *et al.*, The Transition temperature in QCD, *Phys. Rev. D* **74** (2006) 054507, https://doi.org/10.1103/PhysRevD.74.054507.
6. Y. Aoki, S. Borsanyi, S. Durr, Z. Fodor, S. D. Katz, S. Krieg and K. K. Szabo, The QCD transition temperature: results with physical masses in the continuum limit II., *JHEP* **06** (2009) 088 https://doi.org/10.1088/1126-6708/2009/06/088.
7. S. Borsanyi *et al.* [Wuppertal-Budapest], Is there still any T_c mystery in lattice QCD? Results with physical masses in the continuum limit III, *JHEP* **09** (2010) 073 https://doi.org/10.1007/JHEP09(2010)073.
8. A. Bazavov *et al.*, The chiral and deconfinement aspects of the QCD transition, *Phys. Rev. D* **85** (2012) 054503 https://doi.org/10.1103/PhysRevD.85.054503.
9. L. Levkova, QCD at nonzero temperature and density, *PoS* **LATTICE2011** (2011) 011, https://doi.org/10.22323/1.139.0011.
10. P. de Forcrand, J. Langelage, O. Philipsen and W. Unger, Lattice QCD Phase Diagram In and Away from the Strong Coupling Limit, *Phys. Rev. Lett.* **113** (2014) 152002, https://doi.org/10.1103/PhysRevLett.113.152002.
11. T. Bhattacharya *et al.*, QCD Phase Transition with Chiral Quarks and Physical Quark Masses, *Phys. Rev. Lett.* **113** (2014) 082001 https://doi.org/10.1103/PhysRevLett.113.082001.
12. A. Bazavov, H. T. Ding, P. Hegde, F. Karsch, E. Laermann, S. Mukherjee, P. Petreczky and C. Schmidt, Chiral phase structure of three flavor QCD at vanishing baryon number density, *Phys. Rev. D* **95** (2017) 074505, https://doi.org/10.1103/PhysRevD.95.074505.
13. J. N. Guenther, Overview of the QCD phase diagram: Recent progress from the lattice, *Eur. Phys. J. A* **57** (2021) 136, https://doi.org/10.1140/epja/s10050-021-00354-6.
14. S. x. Qin, L. Chang, H. Chen, Y. x. Liu and C. D. Roberts, Phase diagram and critical endpoint for strongly-interacting quarks, *Phys. Rev. Lett.* **106** (2011) 172301, https://doi.org/10.1103/PhysRevLett.106.172301.
15. C. S. Fischer, J. Luecker and J. A. Mueller, Chiral and deconfinement phase transitions of two-flavour QCD at finite temperature and chemical potential, *Phys. Lett. B* **702** (2011) 438, https://doi.org/10.1016/j.physletb.2011.07.039.
16. A. Ayala, A. Bashir, C. A. Dominguez, E. Gutierrez, M. Loewe and A. Raya, QCD phase diagram from finite energy sum rules, *Phys. Rev. D* **84** (2011) 056004, https://doi.org/10.1103/PhysRevD.84.056004.
17. E. Gutierrez, A. Ahmad, A. Ayala, A. Bashir and A. Raya, The QCD phase diagram from Schwinger–Dyson equations, *J. Phys. G* **41** (2014) 075002, https://doi.org/10.1088/0954-3899/41/7/075002.
18. K. l. Wang, Y. x. Liu, L. Chang, C. D. Roberts and S. M. Schmidt, Baryon and meson screening masses, *Phys. Rev. D* **87** (2013) 074038, https://doi.org/10.1103/PhysRevD.87.074038.
19. F. Gao, J. Chen, Y. X. Liu, S. X. Qin, C. D. Roberts and S. M. Schmidt, Phase diagram and thermal properties of strong-interaction matter, *Phys. Rev. D* **93** (2016) 094019, https://doi.org/10.1103/PhysRevD.93.094019.
20. G. Eichmann, C. S. Fischer and C. A. Welzbacher, Baryon effects on the location of QCD's critical end point, *Phys. Rev. D* **93** (2016) 034013, https://doi.org/10.1103/PhysRevD.93.034013.

21. F. Gao and Y. x. Liu, QCD phase transitions via a refined truncation of Dyson-Schwinger equations, *Phys. Rev. D* **94** (2016) 076009, https://doi.org/10.1103/PhysRevD.94.076009.

22. C. S. Fischer, QCD at finite temperature and chemical potential from Dyson–Schwinger equations, *Prog. Part. Nucl. Phys.* **105** (2019) 1, https://doi.org/10.1016/j.ppnp.2019.01.002.

23. C. Shi, X. T. He, W. B. Jia, Q. W. Wang, S. S. Xu and H. S. Zong, Chiral transition and the chiral charge density of the hot and dense QCD matter, *JHEP* **06** (2020) 122, https://doi.org/10.1007/JHEP06(2020)122.

24. A. Ahmad, A. Bashir, M. A. Bedolla and J. J. Cobos-Martínez, Flavor, temperature and magnetic field dependence of the QCD phase diagram: magnetic catalysis and its inverse, *J. Phys. G* **48** (2021) 075002; A. Ahmad and A. Raya, Inverse magnetic catalysis and confinement within a contact interaction model for quarks, *J. Phys. G* **43** (2016) 065002.

25. J. L. Goity and H. Leutwyler, On the Mean Free Path of Pions in Hot Matter, *Phys. Lett. B* **228** (1989) 517, https://doi.org/10.1016/0370-2693(89)90985-4.

26. A. Schenk, Pion propagation at finite temperature, *Phys. Rev. D* **47** (1993) 5138, https://doi.org/10.1103/PhysRevD.47.5138.

27. J. Gasser and H. Leutwyler, Light Quarks at Low Temperatures, *Phys. Lett. B* **184** (1987) 83, https://doi.org/10.1016/0370-2693(87)90492-8.

28. P. Gerber and H. Leutwyler, Hadrons Below the Chiral Phase Transition, *Nucl. Phys. B* **321** (1989) 387, https://doi.org/10.1016/0550-3213(89)90349-0.

29. V. P. Gusynin, V. A. Miransky and I. A. Shovkovy, Dimensional reduction and dynamical chiral symmetry breaking by a magnetic field in (3+1)-dimensions, *Phys. Lett. B* **349** (1995) 477, https://doi.org/10.1016/0370-2693(95)00232-A.

30. D. S. Lee, C. N. Leung and Y. J. Ng, Chiral symmetry breaking in a uniform external magnetic field, *Phys. Rev. D* **55** (1997) 6504, https://doi.org/10.1103/PhysRevD.55.6504.

31. D. K. Hong, Magnetic catalysis in quantum electrodynamics, *Phys. Rev. D* **57** (1998) 3759, https://doi.org/10.1103/PhysRevD.57.3759.

32. E. J. Ferrer and V. de la Incera, Magnetic catalysis in the presence of scalar fields, *Phys. Lett. B* **481** (2000) 287, https://doi.org/10.1016/S0370-2693(00)00482-2.

33. A. Ayala, A. Bashir, A. Raya and E. Rojas, Dynamical mass generation in strongly coupled quantum electrodynamics with weak magnetic fields, *Phys. Rev. D* **73** (2006) 105009, https://doi.org/10.1103/PhysRevD.73.105009.

34. E. Rojas, A. Ayala, A. Bashir and A. Raya, Dynamical mass generation in QED with magnetic fields: Arbitrary field strength and coupling constant, *Phys. Rev. D* **77** (2008) 093004, https://doi.org/10.1103/PhysRevD.77.093004.

35. A. Ayala, A. Bashir, E. Gutierrez, A. Raya and A. Sanchez, Chiral and Parity Symmetry Breaking for Planar Fermions: Effects of a Heat Bath and Uniform External Magnetic Field, *Phys. Rev. D* **82** (2010) 056011, https://doi.org/10.1103/PhysRevD.82.056011.

36. G. S. Bali, F. Bruckmann, G. Endrodi, Z. Fodor, S. D. Katz, S. Krieg, A. Schafer and K. K. Szabo, The QCD phase diagram for external magnetic fields, *JHEP* **02** (2012) 044, https://doi.org/10.1007/JHEP02(2012)044.

37. G. S. Bali, F. Bruckmann, G. Endrodi, Z. Fodor, S. D. Katz and A. Schafer, QCD quark condensate in external magnetic fields, *Phys. Rev. D* **86** (2012) 071502, https://doi.org/10.1103/PhysRevD.86.071502.

38. G. S. Bali, F. Bruckmann, G. Endrodi, F. Gruber and A. Schaefer, Magnetic field-induced gluonic (inverse) catalysis and pressure (an)isotropy in QCD, *JHEP* **04** (2013) 130, https://doi.org/10.1007/JHEP04(2013)130.

39. V. G. Bornyakov, P. V. Buividovich, N. Cundy, O. A. Kochetkov and A. Schäfer, Deconfinement transition in two-flavor lattice QCD with dynamical overlap fermions in an external magnetic field, *Phys. Rev. D* **90** (2014) 034501, https://doi.org/10.1103/PhysRevD.90.034501.

40. V. P. Pagura, D. Gomez Dumm, S. Noguera and N. N. Scoccola, Magnetic catalysis and inverse magnetic catalysis in nonlocal chiral quark models, *Phys. Rev. D* **95** (2017) 034013, https://doi.org/10.1103/PhysRevD.95.034013.

41. A. Ahmad and A. Farooq, Schwinger Pair Production in QCD from Flavor-Dependent Contact Interaction Model of Quarks, [arXiv:2302.13265 [hep-ph]].

42. The Committee on the Assessment of and Outlook for Nuclear Physics; Board on Physics and Astronomy; Division on Engineering and Physical Sciences; National Research Council, *Nuclear Physics: Exploring the Heart of Matter* (National Academies Press, 2012).

43. S. x. Qin, L. Chang, Y. x. Liu and C. D. Roberts, Quark spectral density and a strongly-coupled QGP, *Phys. Rev. D* **84** (2011) 014017, https://doi.org/10.1103/PhysRevD.84.014017.

44. C. E. Detar and J. B. Kogut, Measuring the Hadronic Spectrum of the Quark Plasma, *Phys. Rev. D* **36** (1987) 2828, https://doi.org/10.1103/PhysRevD.36.2828.

45. I. Pushkina *et al.* [QCD-TARO], Properties of hadron screening masses at finite baryonic density, *Phys. Lett. B* **609** (2005) 265, https://doi.org/10.1016/j.physletb.2005.01.006.

46. M. Cheng *et al.* Meson screening masses from lattice QCD with two light and the strange quark, *Eur. Phys. J. C* **71** (2011) 1564, https://doi.org/10.1140/epjc/s10052-011-1564-y.

47. P. Petreczky, Lattice QCD at non-zero temperature, *J. Phys. G* **39** (2012) 093002, https://doi.org/10.1088/0954-3899/39/9/093002.

48. H. L. L. Roberts, L. Chang, I. C. Cloet and C. D. Roberts, Masses of ground and excited-state hadrons, *Few Body Syst.* **51** (2011) 1, https://doi.org/10.1007/s00601-011-0225-x.

49. M. A. Bedolla, J. J. Cobos-Martínez and A. Bashir, Charmonia in a contact interaction, *Phys. Rev. D* **92** (2015) 054031, https://doi.org/10.1103/PhysRevD.92.054031.

50. M. A. Bedolla, K. Raya, J. J. Cobos-Martínez and A. Bashir, η_c elastic and transition form factors: Contact interaction and algebraic model, *Phys. Rev. D* **93** (2016) 094025, https://doi.org/10.1103/PhysRevD.93.094025.
51. K. Raya, M. A. Bedolla, J. J. Cobos-Martínez and A. Bashir, Heavy quarkonia in a contact interaction and an algebraic model: mass spectrum, decay constants, charge radii and elastic and transition form factors, *Few Body Syst.* **59** (2018) 133, https://doi.org/10.1007/s00601-018-1455-y.
52. L. X. Gutiérrez-Guerrero, A. Bashir, M. A. Bedolla and E. Santopinto, Masses of Light and Heavy Mesons and Baryons: A Unified Picture, *Phys. Rev. D* **100** (2019) 114032, https://doi.org/10.1103/PhysRevD.100.114032.
53. P. Boucaud, J. P. Leroy, A. L. Yaouanc, J. Micheli, O. Pene and J. Rodriguez-Quintero, The Infrared Behaviour of the Pure Yang-Mills Green Functions, *Few Body Syst.* **53** (2012) 387, https://doi.org/10.1007/s00601-011-0301-2.
54. D. Binosi, C. Mezrag, J. Papavassiliou, C. D. Roberts and J. Rodriguez-Quintero, Process-independent strong running coupling, *Phys. Rev. D* **96** (2017) 054026, https://doi.org/10.1103/PhysRevD.96.054026.
55. A. Deur, S. J. Brodsky and G. F. de Teramond, The QCD Running Coupling, *Nucl. Phys.* **90** (2016) 1, https://doi.org/10.1016/j.ppnp.2016.04.003.
56. D. Ebert, T. Feldmann and H. Reinhardt, Extended NJL model for light and heavy mesons without q - anti-q thresholds, *Phys. Lett. B* **388** (1996) 154, https://doi.org/10.1016/0370-2693(96)01158-6.
57. C. D. Roberts, Hadron Properties and Dyson-Schwinger Equations, *Prog. Part. Nucl. Phys.* **61** (2008) 50, https://doi.org/10.1016/j.ppnp.2007.12.034.
58. R. L. S. Farias, G. Dallabona, G. Krein and O. A. Battistel, Extension of the Nambu-Jona-Lasinio model at high densities and temperatures using an implicit regularization scheme, *Phys. Rev. C* **77** (2008) 065201, https://doi.org/10.1103/PhysRevC.77.065201.
59. E. E. Salpeter and H. A. Bethe, A Relativistic equation for bound state problems, *Phys. Rev.* **84** (1951) 1232, https://doi.org/10.1103/PhysRev.84.1232.
60. G. S. Bali *et al.* [SESAM], Observation of string breaking in QCD, *Phys. Rev. D* **71** (2005) 114513, https://doi.org/10.1103/PhysRevD.71.114513.
61. L. Chang, I. C. Cloet, B. El-Bennich, T. Klahn and C. D. Roberts, Exploring the light-quark interaction, *Chin. Phys. C* **33** (2009) 1189, https://doi.org/10.1088/1674-1137/33/12/022.
62. A. Bochkarev and J. I. Kapusta, Chiral symmetry at finite temperature: Linear versus nonlinear sigma models, *Phys. Rev. D* **54** (1996) 4066, https://doi.org/10.1103/PhysRevD.54.4066.
63. S. Ferreres-Solé, A. Gómez Nicola and A. Vioque-Rodríguez, Role of the thermal $f_0(500)$ in chiral symmetry restoration, *Phys. Rev. D* **99** (2019) 036018, https://doi.org/10.1103/PhysRevD.99.036018.
64. A. Bender, C. D. Roberts and L. Von Smekal, Goldstone theorem and diquark confinement beyond rainbow ladder approximation, *Phys. Lett. B* **380** (1996) 7, https://doi.org/10.1016/0370-2693(96)00372-3.
65. L. Chang, C. D. Roberts and P. C. Tandy, Selected highlights from the study of mesons, *Chin. J. Phys.* **49** (2011) 955,
66. S. x. Qin, L. Chang, Y. x. Liu, C. D. Roberts and D. J. Wilson, Investigation of rainbow-ladder truncation for excited and exotic mesons, *Phys. Rev. C* **85** (2012) 035202, https://doi.org/10.1103/PhysRevC.85.035202.
67. H. L. L. Roberts, A. Bashir, L. X. Gutierrez-Guerrero, C. D. Roberts and D. J. Wilson, pi- and rho-mesons, and their diquark partners, from a contact interaction, *Phys. Rev. C* **83** (2011) 065206, https://doi.org/10.1103/PhysRevC.83.065206.
68. C. Chen, L. Chang, C. D. Roberts, S. Wan and D. J. Wilson, Spectrum of hadrons with strangeness, *Few Body Syst.* **53** (2012) 293, https://doi.org/10.1007/s00601-012-0466-3.
69. I. S. Gradshteyn and I. M. Ryzhik, *Table of Integrals, Series, and Products* (Academic Press, New York, 1980).